

Triplet State Dissociation of C₁₂₀, the Dimer of C₆₀

Sergei M. Bachilo, Angelo F. Benedetto, and R. Bruce Weisman*

Department of Chemistry, Rice University, Houston, Texas 77005

Received: June 29, 2001

Photophysical and photochemical properties of C₁₂₀, the [2+2]-dimer of C₆₀, have been investigated. In toluene solution, the 327 nm ground-state absorption peak has a molar absorptivity of 113 000 dm³ mol⁻¹ cm⁻¹, somewhat more than twice that of the analogous 336 nm peak of C₆₀. The S₁ and T₁ origin energies in C₁₂₀ are found to be lower than those in C₆₀ by approximately 1070 and 625 cm⁻¹, respectively. The T₁ state's intrinsic exponential lifetime at 296 K is 42 ± 2 μs, or a factor of 3.4 times shorter than for C₆₀. The T_n ← T₁ absorption spectrum of C₁₂₀ shows bands at 710 and 1060 nm. The former is similar to those seen in [6,6]-adducts of C₆₀, but the latter may reflect electronic coupling between the two halves of the dimer molecule. In degassed room-temperature toluene solution, C₁₂₀ photodissociates to C₆₀ with a quantum yield of 2.3 × 10⁻³. This dissociation occurs from the T₁ state and is strongly suppressed by dissolved oxygen. The rate constant for T₁ dissociation increases from ca. 55 s⁻¹ at 297 K to 800 s⁻¹ at 333 K, implying an Arrhenius activation energy near 64 kJ mol⁻¹ (5360 cm⁻¹) and a prefactor in the range of vibrational frequencies.

Introduction

C₁₂₀, the dumbbell-shaped dimer of C₆₀, was first synthesized and structurally characterized by Komatsu and co-workers.¹ In this molecule, the two C₆₀ moieties are bound through [2 + 2]-cycloaddition to give a structure with D_{2h} point group symmetry. The two linking single bonds terminate within each C₆₀ unit on adjacent carbon atoms at the fusion of six-membered rings. In terms of electronic structure, the C₁₂₀ molecule, which contains 116 π-electrons, may be viewed as a dimer of C₆₀ [6,6]-adducts. Studies of triplet relaxation in C₁₂₀ may therefore help clarify the mechanism of self-quenching in encounters between triplet and ground-state fullerene derivatives. C₁₂₀ can also be considered the simplest fullerene oligomer, and it therefore holds substantial interest for investigators trying to understand the properties of larger fullerene oligomers and polymers. The formation mechanisms and characteristics of such polymers and solid-state fullerenes are under active study because of their potential relevance to novel materials having specific electrical or optical properties.^{2–4} Moreover, studies of C₁₂₀ may assist the design of dyad compounds formed from heterofullerenes or derivatized fullerenes that may be tailored for applications involving charge or energy transfer.^{5,6}

C₁₂₀ photophysics research published to date includes a study that found the molecule's ground-state absorption and fluorescence origins at 14 325 and 13 890 cm⁻¹, respectively.⁷ The reported fluorescence quantum yield of 9.2 × 10⁻⁴ and fluorescence lifetime of 1.5 ns are similar to those of other C₆₀ derivatives.⁷ Another study measured the Raman spectrum of solid C₁₂₀.⁸ The triplet state formation quantum yield of C₁₂₀ was found to be 0.7 ± 0.1,⁹ and its lifetime in fluid solution was estimated to be 10 μs in one study and 23 μs in another.^{7,9} Although the T_n ← T₁ absorption spectra reported from those two investigations both showed strong red absorptions, the published spectra do not match in shape or peak position. Finally, the T₁ energy of C₁₂₀ was estimated to lie near 12 000 cm⁻¹ based on quenching rate constants found with a series of triplet energy acceptors.⁹ Theoretical studies have also addressed the electronic and vibrational structures of C₁₂₀.^{10–12}

The photochemical properties of C₁₂₀ have remained poorly characterized. Komatsu et al. observed slow photodissociation to C₆₀ under ambient laboratory light,¹³ but Ma et al. reported that a sample of C₁₂₀ in toluene appeared photostable after 10 h of irradiation with a 450 W Xenon lamp.⁷ Previous work from our laboratory found that C₁₂₀ photodissociates with a quantum yield near 2 × 10⁻³ in degassed toluene solution at room temperature.¹⁴ Most recently, Lebedkin et al. reported photodissociation of C₁₂₀ in both air-saturated and degassed *o*-dichlorobenzene, with quantum yields estimated as 6 × 10⁻⁵ and 7 × 10⁻⁴, respectively.¹⁵

We describe here quantitative studies of C₁₂₀ that clarify the triplet state's intrinsic lifetime, T_n ← T₁ absorption spectrum, energy, and temperature-dependent dissociation. Our results show that C₁₂₀ photodissociation occurs through thermally activated barrier-crossing from the T₁ electronic surface, a view supported by new quantum chemical computations. Isosbestic points in the spectrum of the dissociating dimer have provided a molar absorptivity calibration for the C₁₂₀ UV–vis absorption spectrum. We have also used fluorescence and absorption spectroscopies to locate the S₁ origin energy.

Methods

C₁₂₀ was prepared from C₆₀ with KCN catalyst using the solid-state vibrating ball mill synthesis described by Komatsu and co-workers.¹ After the reaction products were dissolved in *o*-dichlorobenzene, trifluoroacetic acid was added to quench the KCN. The mixture was then filtered and separated by HPLC using toluene mobile phase with a Cosmosil 5PYE column. The resulting C₁₂₀ had a purity greater than 99%.

Samples were dissolved either in toluene or in solid films of poly(methyl methacrylate) (PMMA). We found that photophysical properties unrelated to molecular diffusion were almost identical in these two solvent environments. HPLC grade toluene (Fisher Optima) was used without additional purification, as distillation was not found to alter the results. The solutions in toluene had typical concentrations of 1 to 5 μM for C₁₂₀ and approximately 2 to 10 μM for C₆₀. To prepare a solid film

sample, a toluene solution of the fullerene was mixed with a viscous toluene solution of PMMA (Sigma-Aldrich, average molecular weight 120 000 or 350 000) and applied to a glass substrate. Clear films approximately 200 μm thick were formed after evaporation of the solvent.

For studies from 77 K to slightly above room temperature, samples were placed in a liquid nitrogen cryostat (Oxford Optistat DN) controlled to within 1 K. Fluid samples were studied at temperatures up to 358 K (85 $^{\circ}\text{C}$) using a water-jacketed fused silica cell connected to a circulating thermostated water bath. Samples were held under vacuum, nitrogen gas, or ambient air, depending on the particular experiment.

A small Nd:YAG laser system (New Wave Mini-Lase II) provided nanosecond-scale 532 nm pulses that were used to excite samples for studies of induced absorption, luminescence, and photodissociation. The illuminated sample areas were typically 0.3–0.4 cm^2 . Excitation pulse energies were often restricted to 30 μJ to prevent undesired photodecomposition, and never exceeded 1 mJ. Our transient absorption apparatus used a stabilized tungsten–halogen lamp to generate a probing light beam. Light from this source passed collinearly through the sample cell before entering a computer-controlled monochromator (ISA Triax 180) containing selectable gratings blazed at 1000 nm (600 gr/mm) and 500 nm (1200 gr/mm). Monochromated probe light was then detected by an amplified Si or Ge photodiode connected to a Tektronix TDS-430A oscilloscope that digitized and averaged the waveforms. This apparatus had a time resolution of 0.7 μs and photometric noise below 10^{-5} AU, a level low enough to obtain reliable transient absorption data from dilute, weakly excited samples. We made measurements of 1270 nm O_2 luminescence using the system described above with the probing lamp switched off and the Ge photodiode detector in place. Steady-state absorption and fluorescence spectra were recorded by Cary 4 and Spex Fluorolog 311 instruments, respectively.

We supplemented the experimental studies with PM3 semi-empirical quantum chemical computations performed on a desktop computer running HyperChem v. 5.1. Molecular orbitals of C_{120} were examined after full geometry optimization. We also predicted one-dimensional reaction profiles for the dissociation of C_{120} by computing energy as a function of increasing separation between C_{60} moieties, both on the S_0 and T_1 potential surfaces of C_{120} .

Results and Discussion

Singlet State Properties. Figure 1 compares the ground-state absorption spectra of C_{120} and C_{60} in toluene solution at 296 K. Molar absorptivity values for C_{60} were scaled to match the careful determination of Moravsky et al.,¹⁶ and those for C_{120} were referenced to C_{60} through isosbestic points found in the phototransformation studies discussed below. Compared to the spectrum of C_{60} , that of C_{120} is significantly more diffuse and shows a blue-shift from 336 nm in C_{60} to 327 nm in C_{120} (a 820 cm^{-1} difference) in the position of the most intense UV band that is observable in toluene. The peak molar absorptivity of this band is a factor of 2.1 larger in C_{120} than in C_{60} , suggesting nearly independent, superimposed absorptions by the two halves of the dimer. In agreement with previous reports,^{7,13} C_{120} also shows absorption peaks at 434 and 698 nm, features that are typical of other [6,6]-derivatized C_{60} species. Because each fullerene cage in C_{120} can be electronically excited, one would expect absorptivities approximately twice those of C_{60} . However, the measured absorptivities significantly exceed these values throughout the

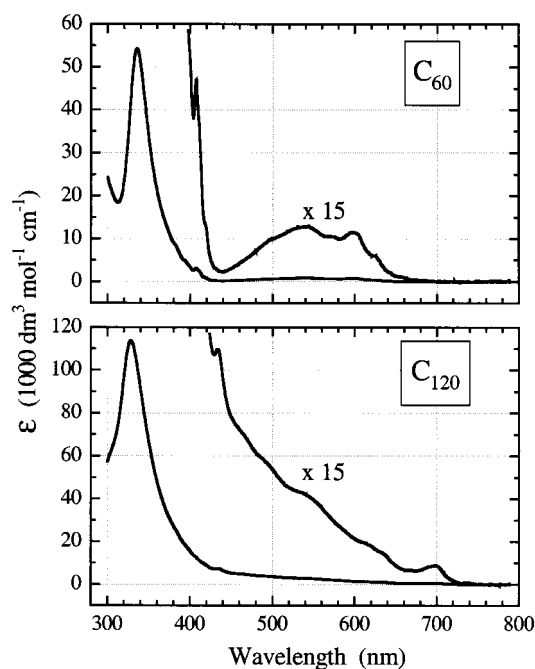


Figure 1. Absorption spectra of C_{60} and C_{120} in toluene at 296 K. The main maximum shifts from 336 nm in C_{60} to 327 nm in C_{120} . Molar absorptivities for C_{60} are taken from the reported peak value of 54 200 $\text{M}^{-1} \text{cm}^{-1}$, and those of C_{120} are measured relative to C_{60} through the method described in the text.

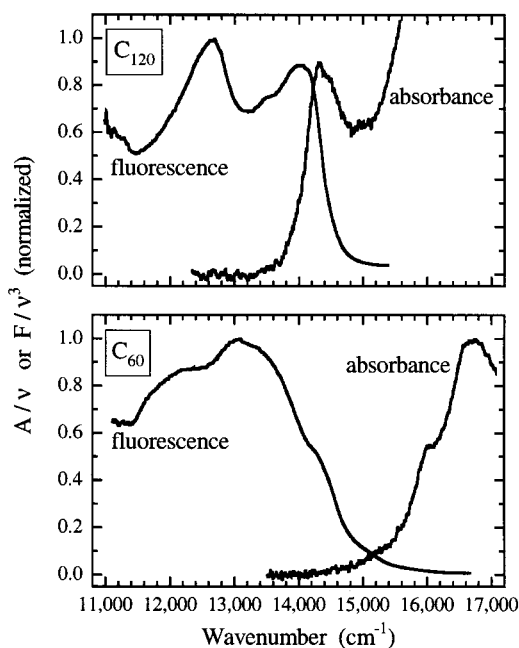


Figure 2. Transformed fluorescence and absorption spectra of C_{60} and C_{120} in toluene at 298 K. The spectra are normalized to reveal mirror-image symmetries near the onsets of absorption and fluorescence.

visible spectral region, probably because of superimposed intracage transitions that are symmetry-forbidden in C_{60} but not in the dimer.

Figure 2 shows the fluorescence spectra of C_{120} and C_{60} , each overlaid with the lowest-energy portion of the corresponding absorption spectrum. To permit a proper comparison between absorption and emission traces, we have divided the absorbance spectrum by frequency (ν), and divided the emission spectrum, expressed in photons per second per unit frequency, by ν^3 .¹⁷ The resulting corrected spectra were then scaled to match the amplitudes of features near the apparent origins. Both frames

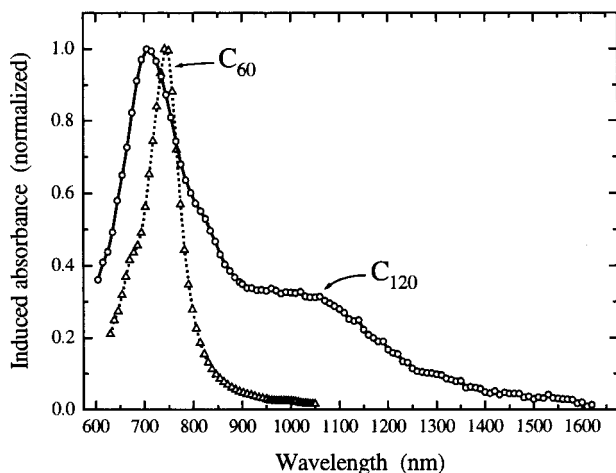


Figure 3. $T_n \leftarrow T_1$ absorption spectra of C₁₂₀ (O, solid line) and C₆₀ (Δ , broken line) in toluene at 298 K. Each spectrum is normalized to its peak value. The main maxima are seen near 710 nm (14 100 cm⁻¹) and 745 nm (13 400 cm⁻¹), respectively.

of Figure 2 show reasonable mirror relations, allowing us to estimate the S₁ origin energies as the crossing points of fluorescence and absorption curves. This gives values of 14 230 (± 70) and 15 300 (± 100) cm⁻¹ for the S₁ origins of C₁₂₀ and C₆₀, respectively. Our C₁₂₀ origin energy is in reasonable agreement with that deduced by Ma et al.⁷ We note that the S₁-S₀ energy gap in C₁₂₀ is lower than in C₆₀ by ca. 1070 cm⁻¹, an amount similar to that found in other [6,6]-closed C₆₀ adducts.¹⁸ It is clear from Figure 2 that the 0-0 bands are relatively much more intense for C₁₂₀ than for C₆₀. The likely explanation is that the transition is symmetry-forbidden in the icosahedral point group of C₆₀ but not in the D_{2h} point group of C₁₂₀.

Triplet State Properties. Reliable measurements of triplet-triplet absorption and kinetics are hampered by the tendency of C₁₂₀ to photodissociate from its T₁ state, as described below. To suppress this problem, we measured transient spectra at early delays in samples that had not been degassed and thus were relatively photostable because of oxygen quenching of the triplet state. Figure 3 shows the induced absorbance spectrum obtained from such a sample of C₁₂₀ in toluene at 298 K over the range from 600 to 1600 nm following excitation at 532 nm. The main feature in this T_n ← T₁ spectrum is the peak at 710 nm, which is broadened and blue-shifted compared to the corresponding peak of C₆₀. This feature, and the weak shoulder near 830 nm, are familiar from the triplet absorption spectra of other [6,6]-derivatives of C₆₀.¹⁹ However, C₁₂₀ also shows a new, broad triplet absorption near 1060 nm that was not clearly revealed in a prior triplet spectrum of C₁₂₀,⁹ and is not seen in simple C₆₀ derivatives.²⁰ We find that this 1060 nm absorption becomes more distinct when the C₁₂₀ is cooled to 100 K in PMMA films. Our T_n ← T₁ spectrum differs significantly from that reported by Ma et al.,⁷ whose samples may have been partly photolyzed to C₆₀ during measurement.

The quantum yield for triplet state formation was investigated by comparing the intensities of ¹O₂ luminescence from absorbance-matched samples of C₁₂₀ and C₆₀ photoexcited in the presence of dissolved oxygen. Assuming the yield for C₆₀ to be 1, the results indicate a value of 0.85 \pm 0.15 for Φ_T of C₁₂₀. (The relatively large uncertainty arises from the low solubility of C₁₂₀ in toluene and the corresponding weakness of ¹O₂ luminescence.) Fujitsuka et al. reported this triplet quantum yield to be 0.7 \pm 0.1, a value consistent with our result within the experimental uncertainties.⁹ On the basis of our

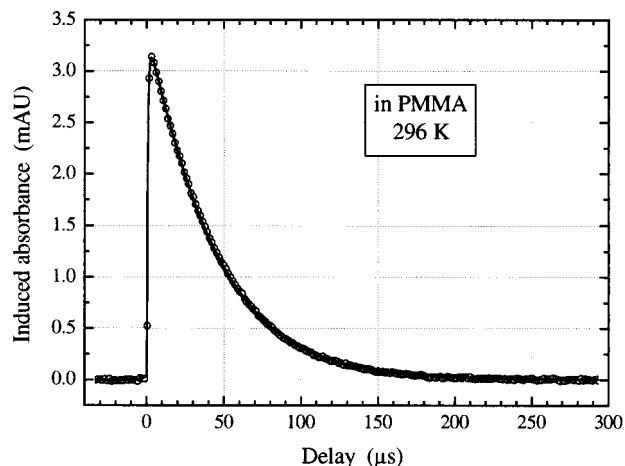


Figure 4. Induced absorption kinetics showing triplet state population decay for C₁₂₀ dissolved in a PMMA film at 296 K. The sample was excited at 532 nm and probed at 1100 nm. The solid curve through the data points shows a simulated first-order decay with an exponential lifetime of 42 μ s.

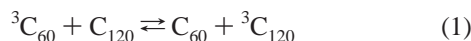
quantum yield result and measured induced absorbance magnitudes, we estimate that the T_n ← T₁ peak molar absorptivity of C₁₂₀ (at 710 nm) is approximately 10 000 dm³ mol⁻¹ cm⁻¹, or a factor of 2 lower than the 19 500 dm³ mol⁻¹ cm⁻¹ absorptivity of T₁ C₆₀ at 745 nm. Because of its greater width, the C₁₂₀ triplet absorption has an oscillator strength in the same range as that of C₆₀, reflecting the fact that only one of the two fullerene cages in C₁₂₀ is electronically excited in the T₁ state. By contrast, both halves of C₁₂₀ contribute to its ground state absorption, and its ground state absorptivity is approximately twice that of C₆₀.

To find the intrinsic T₁ lifetime of C₁₂₀ without interference from photoproducts formed during the measurement, we have used two approaches. In the first, we measured induced absorption kinetics near 710 nm following a single relatively strong excitation pulse in a freshly prepared sample. The resulting trace, which showed a peak induced signal of 22 mAU, was analyzed as a mixture of concurrent first- and second-order decays to obtain a first-order lifetime of 44 \pm 2 μ s in room-temperature toluene. In our second approach, we averaged data over many weaker excitation pulses but shifted the probing wavelength to 1100 nm to minimize the relative contribution of the C₆₀ photoproduct. Figure 4 shows such a kinetic trace for a sample of C₁₂₀ dissolved in a thin film of PMMA. The data fit well to a first-order model with an exponential decay time of 42 \pm 1 μ s. We obtained equivalent results on samples in toluene solution at 297 K. Emission measurements made on 80 K film samples showed unusually broad phosphorescence extending from ca. 730 nm to beyond 860 nm. We found that the phosphorescence detected at 840 nm showed a decay profile matching the kinetics of transient absorption. From these results, we confidently conclude that the intrinsic T₁ lifetime of C₁₂₀ near room temperature is 42 \pm 2 μ s. This value substantially exceeds the 10 μ s lower limit estimated by Ma et al.,⁷ and it differs significantly from the 23 μ s lifetime reported by Fujitsuka et al.⁹

When compared to the 142 μ s lifetime of C₆₀ under the same conditions,¹⁹ our finding indicates that triplet state decay is accelerated by a factor of approximately 3.4 in the dimer. The very similar accelerations measured for simpler [6,6]-adducts of C₆₀ support the view that the triplet excitation in C₁₂₀ is effectively localized on one-half of the molecule.¹⁹ Moreover, the unexceptional lifetime of C₁₂₀ suggests that the triplet-excited

half undergoes little intramolecular self-quenching by the unexcited half. We found a weak temperature dependence in the triplet state decay of C_{120} , as its lifetime at 77 K (in PMMA) was only 65 μs , a value about 3.6 times shorter than the 238 μs triplet lifetime of C_{60} at that temperature. In air-saturated toluene solutions, the triplet state decays of C_{60} and C_{120} differed by less than 5%, indicating very comparable diffusion-controlled quenching of their T_1 states by molecular oxygen.

Analysis of the weak and broad phosphorescence spectrum did not allow us to determine the T_1 energy of C_{120} . In an alternative approach, we studied the induced absorption kinetics of a solution phase sample containing a mixture of C_{60} and C_{120} . Such mixtures support the bimolecular transfer of triplet excitation between species, leading to characteristic kinetic profiles that can be analyzed to deduce the ratio of forward to reverse energy transfer rate constants. We applied a kinetic model, used earlier in this laboratory, that includes independent first-order depopulation of the two fullerene species and bimolecular energy transfer between them.²¹ Figure 5 shows induced absorbance data measured at 900 nm for a sample containing 4 μM C_{120} and 15 μM C_{60} in toluene at 296 K. The shape from 0 to 50 μs is notably nonexponential because of triplet energy transfer between the two fullerenes. The measured kinetic trace is well simulated by the solid curve, which was computed using the kinetic model outlined above with first-order decay constants determined independently. The bottom frame of Figure 5 shows the absence of systematic trends in the difference between measured and simulated kinetic data. By combining the ratio of energy transfer rate constants deduced in this optimized simulation with the known ratio of fullerene concentrations in the sample, we find a triplet state equilibrium constant of 7.5 ± 2.5 for the reaction



We then assume that the entropy change in this reaction is dominated by the different triplet state orbital degeneracies of C_{60} and C_{120} (3 vs 1), giving $\Delta S^0 = -9.1 \text{ J mol}^{-1} \text{ K}^{-1}$. Combining this value with the ΔG^0 result corresponding to the measured equilibrium constant, we find that ΔH^0 is $-625 \pm 100 \text{ cm}^{-1}$. Because this equals the T_1 energy in C_{120} relative to that in C_{60} , our analysis places the T_1 - S_0 gap of C_{120} at approximately $12\,000 \pm 100 \text{ cm}^{-1}$. This value is consistent with the less precise determination of Fujisuka et al. based on quenching by different triplet energy acceptors.⁹ We note that similar T_1 energies of approximately $12\,100 \text{ cm}^{-1}$ have been reported from phosphorescence measurements on C_{60} mono-adducts having 3-, 5-, and six-membered rings external to the cage.²² However, in 1,2-(CH_3) $_2C_{60}$, which is an acyclic [6,6]-closed derivative, the T_1 energy was found to lie only 285 cm^{-1} below that of the parent C_{60} .²³ We conclude that dimerization of C_{60} to form C_{120} lowers the T_1 origin energy by about the same amount as in other cyclic [6,6]-derivatives but by more than in some acyclic derivatives.

Photodissociation. In agreement with some earlier reports,^{13,15} but in contrast to others,^{7,24} we find that solutions of C_{120} are unstable in the presence of light. Our HPLC and spectrophotometric analyses show that C_{60} is the only detectable product of oxygen-free C_{120} photolysis. To quantify this process, we have monitored the changing UV-vis absorption spectra of C_{120} samples during exposure to photolyzing light. Figure 6 shows several spectra from such a series measured in a degassed toluene solution irradiated for a total of 3600 s with 345 nm light from a monochromated xenon lamp. The C_{120}

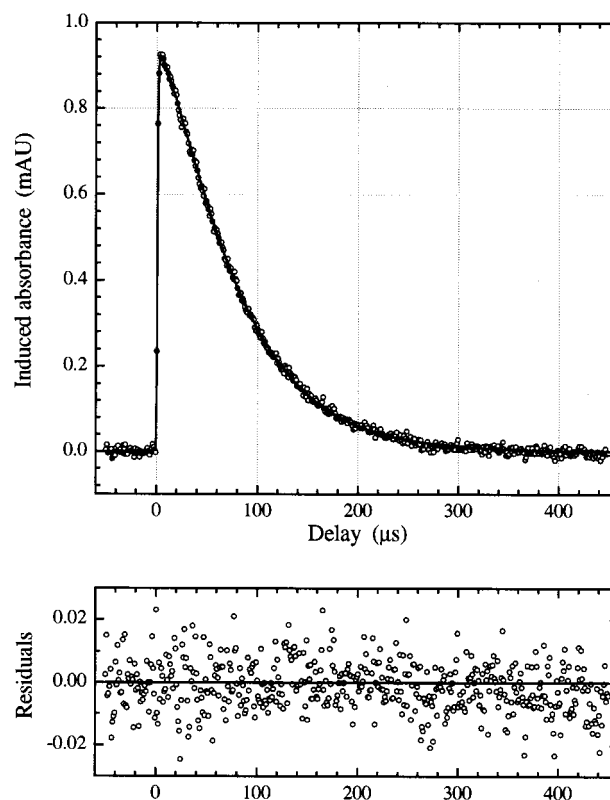


Figure 5. Induced absorbance measured at 900 nm for a mixed solution of 4 μM C_{120} plus 15 μM C_{60} in toluene at 296 K following excitation at 532 nm. The solid curve is a kinetic simulation computed using the model and parameters described in the text. The lower frame shows differences (in mAU) between the data and this simulation.

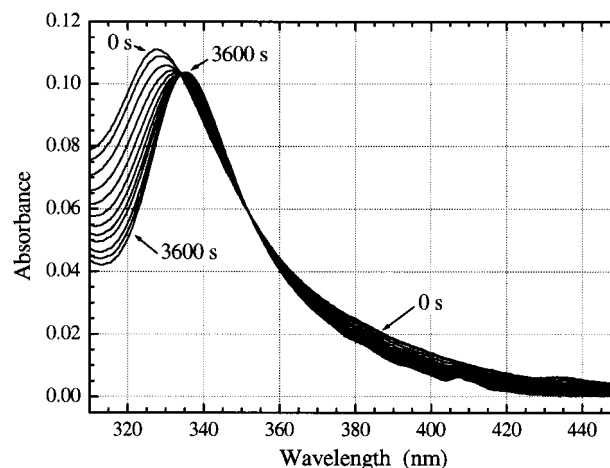


Figure 6. Changing electronic absorption spectrum of a degassed sample of C_{120} in toluene as it dissociated to C_{60} during 3600 s of irradiation at 345 nm. The intervals between plotted traces are not constant.

peaks at 327 and 434 nm evolve into those of C_{60} at 336 and 407 nm. In addition, isobestic points are clearly visible at 334 and 352 nm, indicating that only one step of photoconversion occurs on the time scale of our observations. Because C_{60} is the sole product, the absorption spectrum of C_{120} can be accurately calibrated for molar absorptivity by matching its values at the isobestic wavelengths to twice those of the well-known C_{60} spectrum. This method was used in preparing Figure 1.

Kinetic analysis of data such as shown in Figure 6 reveals matching first-order rate constants for the loss of C_{120} and the formation of C_{60} . To determine Φ_{diss} , the quantum yield of

photodissociation, we write

$$\Phi_{\text{diss}} = \frac{dN_{120}}{dN_{\text{ph}}} = \frac{\{dN_{120}\}/\{dt\}}{\{dN_{\text{ph}}\}/\{dt\}} \quad (2)$$

where N_{120} is the number of reactant molecules and N_{ph} is the number of excitation photons. Denoting the incident excitation power by P_{exc} , and the excitation optical frequency by ν_{exc} , and writing the fractional absorption of excitation photons by the reactant in our optically thin sample as $1 - T \cong 2.303\epsilon l[C_{120}]$, one obtains

$$\frac{dN_{\text{ph}}}{dt} = \frac{-2.303\epsilon l[C_{120}]P_{\text{exc}}}{h\nu_{\text{exc}}} \quad (3)$$

The numerator of eq 2 is easily re-expressed in concentration units

$$\frac{dN_{120}}{dt} = VN_{\text{Av}} \frac{d[C_{120}]}{dt} \quad (4)$$

where N_{Av} is Avogadro's number, and V is the sample volume. Substituting eq 3 and 4 into eq 2, separating variables, and integrating gives

$$\Phi_{\text{diss}} = \frac{kVN_{\text{Av}}h\nu_{\text{exc}}}{2.303P_{\text{exc}}\epsilon l} \quad (5)$$

Here, k is the measured first-order rate constant for reactant loss under constant sample irradiation. Evaluating this expression with our data for C₁₂₀ in degassed toluene at 297 K, we find a photodissociative quantum yield of 2.2×10^{-3} . This quantum yield is reduced by at least 2 orders of magnitude in air-saturated solution, strongly suggesting that dissociation of C₁₂₀ occurs from the oxygen-quenchable T₁ state. Our value for the oxygen-free quantum yield is approximately three times greater than that reported by Lebedkin et al. for C₁₂₀ in *o*-dichlorobenzene.¹⁵

The photodissociative quantum yield also depends strongly on temperature. To study this dependence, we measured Φ_{diss} using a different method based on our finding that the induced absorption of C₁₂₀ is at least 20 times greater than that of C₆₀ at wavelengths near 1050 nm. We measured the changing magnitude of 1050 nm induced absorbance in degassed C₁₂₀ solutions as they were exposed to 532 nm laser pulses, which both photolyzed the sample and also generated the triplet states whose absorption was probed. As the C₁₂₀ concentration declined through photolysis, the measured peak induced absorption declined dramatically. By analyzing the rate of this decay in thermostated samples, we found that Φ_{diss} increases from 2.2×10^{-3} to 3.7×10^{-2} over the range from 297 to 333 K.

We have divided these temperature-dependent Φ_{diss} values by the corresponding T₁ lifetimes to obtain rate constants for dissociation of C₁₂₀ from its T₁ state. Over the studied temperature range, the dissociation constant ranges from approximately 55 to 800 s⁻¹. (Our analysis assumes a temperature-independent triplet quantum yield of 1, although errors in this assumption will have only minor effects on the results.) Figure 7 shows dissociative rate constants plotted in Arrhenius form with a linear best fit and 95% confidence bands. The slope in Figure 7 gives an activation energy for triplet state dissociation of 64 ± 5 kJ mol⁻¹ (5360 ± 400 cm⁻¹). The Arrhenius prefactor found from the intercept is approximately 9×10^{12} s⁻¹, corresponding to an attempt frequency near 300 cm⁻¹ (95% confidence limits: 50 to 1700 cm⁻¹) These values indicate that once a C₁₂₀ molecule reaches its T₁ state, it can dissociate

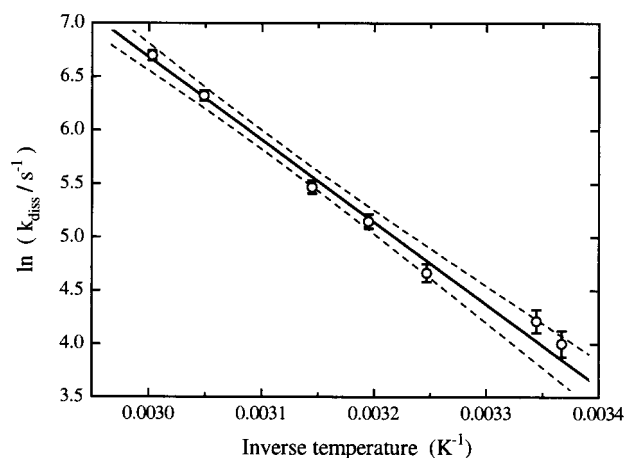


Figure 7. Temperature dependence of the dissociative rate constant for the T₁ state of C₁₂₀, plotted in Arrhenius form. The solid line is a linear least-squares fit, with upper and lower confidence limits shown by dashed lines.

through vibrational motion over a relatively small potential barrier. Although our measurements do not reveal the electronic states of the two product C₆₀ molecules, spin conservation considerations suggest that one is formed in the T₁ state and the other in S₀.

To compare the dissociative properties of the T₁ and S₀ states, we have also investigated the thermolysis of C₁₂₀. Less than ca. 3% dissociation was detected in dark C₁₂₀ samples held for several hours at 85 °C. This implies that dissociation from the ground electronic state is slower than from the triplet state by a factor of at least 3×10^8 . If these processes have similar prefactors, the ground-state activation barrier would be greater than the T₁ barrier by at least 5000 cm⁻¹ (60 kJ mol⁻¹), placing its value above 10 000 cm⁻¹ (120 kJ mol⁻¹). This estimate is consistent with the 14 000 cm⁻¹ activation energy reported for dissociation of solid C₁₂₀.³

Computational Findings

Our semiempirical quantum computations provide a qualitative explanation for the lowered triplet state dissociation barrier. Excitations to the S₁ and T₁ state of C₁₂₀ correspond to a one-electron promotion from HOMO to LUMO. Our computations reveal that the HOMO has a high bonding electron density between the two C₆₀ moieties, whereas the LUMO (as well as the nearby LUMO + 1) orbital has almost no electron density on those bonds linking the dimer's halves. Thus, transitions from S₀ to S₁ or T₁ weaken the bonds that must break during dissociation of C₁₂₀. Further theoretical confirmation of this conclusion comes from calculations of the molecular energy as a function of distance between the C₆₀ moieties. These curves show a dissociation barrier that is approximately 8000 cm⁻¹ (100 kJ mol⁻¹) lower on the triplet than on the ground-state surface.

Dissociation of C₁₂₀ likely occurs along a mixture of normal mode coordinates. In agreement with prior experimental and computational work,^{8,10,11} our PM3 analysis of S₀ vibrations shows that the mode observed in the Raman spectrum at 96 cm⁻¹ involves a large displacement in the distance between centers of the C₆₀ cages, although with little change in the bonds linking the cages. Another normal mode, found computationally at 1017 cm⁻¹, shows strong changes in the lengths of both linking bonds, along with complementary changes in the lengths of adjacent cage bonds. Some combination of such modes probably forms the dissociation coordinate, but the uncertainty

in our experimental T_1 Arrhenius prefactor prevents a more precise identification.

Computations can also provide some insight into the extent of electronic interaction between the two C_{60} moieties of C_{120} . As expected, our PM3 results show that C_{120} molecular orbitals can be identified as symmetric and antisymmetric combinations of C_{60} -adduct orbitals. Electronic interactions between the two C_{60} π -systems cause splittings between such pairs ranging from ca. 0.01 eV to 0.3 eV, depending on the orbitals' shape and orientation. These couplings would enable rapid exchange of energy or electrons between the two C_{60} cages. Such splittings may cause the UV-vis electronic absorption spectrum to be broader for C_{120} than for other simple derivatives of C_{60} . Another consequence may be evident in the intriguing $T_n \leftarrow T_1$ band near 1050 nm, which does not seem to be present in other [6,6]-closed adducts of C_{60} .²⁰

Conclusions

We have further characterized the photophysical and photochemical properties of C_{120} , the dimer of C_{60} . As is common for [6,6]-adducts of C_{60} , the S_1 and T_1 origin energies of C_{120} are significantly lowered from those of C_{60} , and the near-ultraviolet absorption peak is shifted several nanometers to shorter wavelength compared to the corresponding peak in C_{60} . The molar absorptivity at this peak is slightly more than twice the value of the C_{60} peak. Following optical excitation, C_{120} forms its T_1 state with a quantum yield not far below 1. The triplet state's intrinsic unimolecular lifetime at room temperature is 42 μ s, a value typical of mono-derivatized C_{60} compounds and substantially shorter than for C_{60} . In addition to a 710 nm peak similar to those in the $T_n \leftarrow T_1$ absorption spectra of other C_{60} monoadducts, the C_{120} triplet spectrum shows an unfamiliar band at 1060 nm that may reflect weak electronic coupling between the two halves of the dimer molecule. There is otherwise little photophysical evidence of electronic interaction between C_{60} moieties in the dimer.

We find that C_{120} photodissociates from its T_1 state in oxygen-free toluene solution, yielding C_{60} as the sole photoproduct. The photodissociation yield and rate constant are strongly temperature dependent, implying an Arrhenius activation energy near 5360 cm^{-1} and a prefactor in the range of molecular vibrational frequencies. Thermal dissociation of C_{120} on the S_0 surface is more than 8 orders of magnitude slower, probably because of a much larger activation barrier. The lower triplet state barrier to C_{120} dissociation is consistent with quantum chemical results that show weakened bonding between the two C_{60} moieties in the T_1 state.

Acknowledgment. We thank Prof. K. Komatsu for generously providing a comparison sample of C_{120} . This research was supported by the National Science Foundation (Grant No. CHE-9900417) and the Robert A. Welch Foundation.

References and Notes

- (1) Wang, G.-W.; Komatsu, K.; Murata, Y.; Shiro, M. *Nature* **1997**, *387*, 583.
- (2) Sundqvist, B. *Adv. Phys.* **1999**, *48*, 1.
- (3) Nagel, P.; Pasler, V.; Lebedkin, S.; Soldatov, A.; Meingast, C.; Sundqvist, B.; Persson, P.-A.; Tanaka, T.; Komatsu, K.; Buga, S.; Inaba, A. *Phys. Rev. B* **1999**, *60*, 16 920.
- (4) Inaba, A.; Matsuo, T.; Fransson, Å.; Sundqvist, B. *J. Chem. Phys.* **1999**, *110*, 12 226.
- (5) Hummelen, J. C.; Knight, B. W.; Pavlovich, J.; Gonzalez, R.; Wudl, F. *Science* **1995**, *269*, 1554.
- (6) Yu, G.; Gao, J.; Hummelen, J. C.; Wudl, F.; Heeger, A. J. *Science* **1995**, *270*, 1789.
- (7) Ma, B.; Riggs, J. E.; Sun, Y.-P. *J. Phys. Chem. B* **1998**, *102*, 5999.
- (8) Lebedkin, S.; Gromov, A.; Giesa, S.; Gleiter, R.; Renker, B.; Rietschel, H.; Kratschmer, W. *Chem. Phys. Lett.* **1998**, *285*, 210.
- (9) Fujitsuka, M.; Luo, C.; Ito, O.; Murata, Y.; Komatsu, K. *J. Phys. Chem. A* **1999**, *103*, 7155.
- (10) Adams, G. B.; Page, J. B.; Sankey, O. F.; O'Keeffe, M. *Phys. Rev. B* **1994**, *50*, 17 471.
- (11) Porezag, D.; Pederson, M. R.; Frauenheim, Th.; Kohler, Th. *Phys. Rev. B* **1995**, *52*, 14 963.
- (12) Osawa, S.; Sakai, M.; Osawa, E. *J. Phys. Chem. A* **1997**, *101*, 1378.
- (13) Komatsu, K.; Wang, G.-W.; Murata, Y.; Tanaka, T.; Fujiwara, K.; Yamamoto, K.; Saunders, M. *J. Org. Chem.* **1998**, *63*, 9358.
- (14) Benedetto, A. F.; Bachilo, S. M.; Weisman, R. B. *Proc. Electrochem. Soc.* **1999**, *99-12*, 381.
- (15) Lebedkin, S.; Hull, W. E.; Soldatov, A.; Renker, B.; Kappes, M. M. *J. Phys. Chem. B* **2000**, *104*, 4101.
- (16) Moravsky, A. P.; Fursikov, P. V.; Kachapina, L. M.; Khramov, A. V.; Kiryakov, N. V. *Proc. Electrochem. Soc.* **1995**, *95-10*, 156.
- (17) Stepanov, B. I.; Gribkovskii, V. P. *Theory of Luminescence*; Iliffe: London, 1968.
- (18) Sun, Y.-P.; Riggs, J. E.; Guo, Z.; Rollins, H. W. Photoexcited state and electron-transfer properties of fullerenes and related materials, In *Optical and Electronic Properties of Fullerenes and Fullerene-Based Materials*; Shinar, J.; Vardeny, Z. V., Kafafi, Z. H., Eds.; Marcel Dekker: New York, 2000; pp 43-81.
- (19) Weisman, R. B. Optical studies of fullerene triplet states, In *Optical and Electronic Properties of Fullerenes and Fullerene-Based Materials*; Shinar, J.; Vardeny, Z. V.; Kafafi, Z. H., Eds.; Marcel Dekker: New York, 2000; pp 83-117.
- (20) Luo, C.; Fujitsuka, M.; Watanabe, A.; Ito, O.; Gan, L.; Huang, Y.; Huang, C.-H. *J. Chem. Soc., Faraday Trans.* **1998**, *94*, 527.
- (21) Fraelich, M. R.; Weisman, R. B. *J. Phys. Chem.* **1993**, *97*, 11 145.
- (22) Guldi, D. M.; Asmus, K.-D. *J. Phys. Chem. A* **1997**, *101*, 1472.
- (23) Ausman, K. D.; Weisman, R. B. *J. Am. Chem. Soc.* **1999**, *121*, 1110.
- (24) Cho, H. S.; Kim, S. K.; Kim, D.; Fujiwara, K.; Komatsu, K. *J. Phys. Chem. A* **2000**, *104*, 9666.